# On the taxonomic identity of *Pteronotus davyi incae* Smith, 1972 (Chiroptera: Mormoopidae)

ANA CAROLINA PAVAN,[1] RICHARD CADENILLAS,[2] OSCAR CENTTY,[3] VÍCTOR PACHECO,[3] AND PAÚL M. VELAZCO[4]

## ABSTRACT

The subgenus *Pteronotus* (naked-backed bats) comprises three species, *P. davyi*, *P. fulvus*, and *P. gymnonotus*, which are distinguished from other members of the genus *Pteronotus* by wing membranes that are fused along the dorsal midline and by skulls with noticeably upturned rostrums. *Pteronotus davyi* currently includes two morphologically differentiated subspecies, *P. d. davyi* and *P. d. incae,* with strikingly disjunct geographic ranges. Whereas the nominotypical form is found in Central America, the Caribbean coastal region of northern South America, and the Lesser Antilles, the subspecies *P. d. incae* is restricted to a small area in northwestern Peru; to date, the phylogenetic relationships of these nominal taxa have not been explored. In the present contribution, we employed analyses of mitochondrial gene sequences, morphometrics, and qualitative-morphological comparisons to provide new information on *P. d. incae* and place the taxon in a phylogenetic context. Our results suggest that the geographically disjunct populations of *P. davyi* are genetically very similar even though they are morphologically and ecologically distinct. Recognizing that speciation is a process with intermediate stages that merit formal recognition, we support the retention of *incae* as a valid subspecies of *Pteronotus davyi*.

[1] Laboratório de Mamíferos, Escola Superior de Agricultura "Luiz de Queiroz" (ESALQ), Universidade de São Paulo, Brazil.

[2] Universidad Austral de Chile, Chile; and Instituto de Paleontología, Universidad Nacional de Piura, Peru.

[3] Departamento de Mastozoología, Museo de Historia Natural, Universidad Nacional Mayor de San Marcos, Peru.

[4] Department of Biology, Arcadia University, Glenside, PA; and Division of Vertebrate Zoology (Mammalogy), American Museum of Natural History, New York.

INTRODUCTION

The Neotropical genus *Pteronotus* Gray, 1838, is represented by a group of small to medium-sized bats distributed from Mexico to central Brazil and into the Caribbean (Pavan, 2019; Pavan and Marroig, 2017). These bats feed exclusively on insects and occupy a wide variety of habitats across their range, from arid and semiarid regions to coastal lowlands and humid forests (Herd, 1983; Patton and Gardner, 2008; Pavan, 2019). Bats in the genus *Pteronotus* has gone through several taxonomic changes, with its recognized species diversity more than doubling in the last decade; the most recent taxonomic arrangement recognizes 16 extant species, grouped into four subgenera or clades (Pavan and Marroig, 2016; Pavan et al., 2018). The subgenus *Pteronotus* currently includes three species, *Pteronotus davyi*, *P. fulvus*, and *P. gymnonotus* (Pavan and Marroig, 2016). These bats form a distinctive morphological group characterized by wing membranes fused dorsally at the midline (giving the back a naked appearance); pointed ears, with a smooth anteromedial edge (lacking serrations); skull rostrum noticeably upturned in lateral profile, and shorter than one-half the total length of the skull; braincase oblong; and basioccipital region broad between the auditory bullae (Smith, 1972; Pavan and Tavares, 2020).

Historically, *Pteronotus fulvus* was considered a subspecies of *P. davyi*, as defined by Smith (1972; referred to as *P. davyi*, sensu lato, hereafter), along with two other subspecies, the nominal *P. d. davyi*, and *P. d. incae*. Nevertheless, molecular and morphometric studies have shown that *P. davyi*, sensu lato. represents a species complex, supporting the elevation of *fulvus* to the species level (Dávalos, 2006; Pavan and Marroig, 2016). Therefore, *P. davyi*, sensu stricto, (referred to as *P. davyi* hereafter) was left including two subspecies: *P. d. davyi*, which is currently known from the coastal lowlands of Venezuela and Colombia northward to Costa Rica and Nicaragua, including several islands in the Lesser Antilles and on the Pacific coast of Panama (Ibáñez et al., 1997; Estrada-Villegas et al., 2018; Pavan, 2019); and *P. d. incae*, represented by populations occurring in northwestern Peru (Smith, 1972; Pavan and Marroig, 2016). There is a considerable gap of more than 1300 km between the populations of these putative subspecies, and *P. d. incae* is easily discernible from specimens of *P. d. davyi* based on its larger cranial and external size (Smith, 1972). The morphometric distinctiveness and geographic isolation might be evidence that *P. d. incae* represents a valid species, but the lack of molecular information precluded previous investigations to assess the phylogenetic status of this taxon (Dávalos, 2006; Pavan and Marroig, 2016, 2017). In the present contribution, we provide new information on *P. d. incae*, including DNA sequence data, and place the taxon in a phylogenetic context, improving our understanding of species diversity and distributional patterns of mormoopid bats.

MATERIAL AND METHODS

Our study employed analyses of mitochondrial gene sequences, morphometrics, and standard morphological comparisons. The specimens examined and the new sequence data generated by this study were from the following collections:

AMNH American Museum of Natural History, New York, New York
BM Natural History Museum, London (formerly the British Museum [Natural History]), London, UK
FMNH Field Museum of Natural History, Chicago, Illinois
KU Biodiversity Institute and Natural History Museum, University of Kansas, Lawrence, Kansas
LACM Los Angeles County Museum of Natural History, Los Angeles, California
MCZ Museum of Comparative Zoology, Harvard, Massachusetts
MUSM Museo de Historia Natural de la Universidad Nacional Mayor de San Marcos, Lima, Peru
MVZ Museum of Vertebrate Zoology, Berkeley, California
NMNH National Museum of Natural History, Smithsonian Institution, Washington, D.C.
ROM Royal Ontario Museum, Toronto, Ontario, Canada
TCWC Texas A&M University, College Station, Texas
TTU, TK Museum of Texas Tech University, Lubbock, Texas

## Molecular Analyses

Sequences from two mitochondrial markers, the cytochrome *b* (cyt-*b*) and cytochrome oxidase I (CO1) genes, were generated for four Peruvian specimens of *P. d. incae*, two from the department of Cajamarca, and two from the department of Piura. These individuals were compared with specimens of *P. davyi* from other localities in the species geographic range, regarded as *P. d. davyi* (fig. 1). Our molecular investigation additionally included sequences of the species *P. fulvus* and *P. gymnonotus*, other members of the subgenus *Pteronotus* together with *P. davyi*. Lastly, we included sequences from representatives of some of the other species within the genus *Pteronotus* and *Mormoops* published by Pavan and Marroig (2016) and available from GenBank, which were used as outgroups in the phylogenetic analyses (appendix 1).

Total genomic DNA was extracted from ethanol-preserved tissues using the Qiagen DNeasy Blood and Tissue Kit (Qiagen, Inc., Germantown, MD). The amplification and sequencing of the cyt-*b* and CO1 fragments were performed using the same primers and conditions described by Pavan and Marroig (2016). Sequences were assembled and checked for quality using Geneious v.9.1 (Biomatters, Ltd., Auckland, New Zealand) and aligned with the sequences already available from GenBank using MEGA6 (Tamura et al., 2013). Phylogenetic analyses were performed on each marker separately and then on the concatenated dataset. Nucleotide substitution models that best explained the variation observed in each dataset were estimated in MEGA6 and used for subsequent analysis. We inferred the relationships among individuals in Mr. Bayes 3.2.6 (Ronquist and Huelsenbeck, 2003) using four Markov chain Monte Carlo (MCMC) analyses in two independent runs at 5 million generations each for single-marker datasets, and 10 million generations for the concatenated dataset. Sampling of chains occurred every 1000 generations and the first 25% of the sampled trees and estimated parameters were discarded as burn-in. Stationarity of runs were checked in Tracer v.1.6 (Rambaut et al., 2014)

FIGURE 1. Map showing the geographic range of *Pteronotus davyi* (shaded green) and the localities sampled in the molecular (red) analyses, morphometric (blue) analyses, or both (black). *P. d. davyi* localities are represented by circles and *P. d. incae* by triangles.

by examining the average standard deviation of split frequencies (Ronquist et al., 2011). Molecular-diversity indices and estimates of genetic differentiation between the lineages were calculated by MEGA7 and DnaSP v5 (Librado and Rozas, 2009). We estimated the relationships among haplotypes using the median-joining network algorithm (Bandelt et al., 1999) by Network 5.0 (fluxus-engineering.com).

## Morphometric and Morphological Analyses

We examined 40 cranial variables (linear distances) of 245 museum specimens: 158 individuals of *P. fulvus*, 71 of *P. d. davyi* and 16 of *P. d. incae* (appendix 2). The distances used in the morphometric analyses were obtained from 22 cranial landmarks collected from the skull of *Pteronotus* species (for additional information, see Pavan and Marroig, 2016: fig. 2, table S4).

Our morphometric dataset included the four specimens of *P. d. incae* for which we have obtained molecular information and two specimens from the type series of *P. d. incae* (TCWC11639 and 11640). We performed a principal component analysis (PCA) to explore the total cranial variation of each species in the multivariate space and to evaluate which morphological variables contributed most to such variation. Discriminant function analysis (DFA) was further used to compare the three defined morphological groups—*P. fulvus* and the two subspecies of *P. davyi*—and to better understand the differences in the cranial morphology within and between the species. All morphometric analyses were performed in the software PAST (Hammer et al., 2001).

We have also evaluated external and osteological characters including, but not restricted to, those defined by Smith (1972) and Pavan et al. (2018) in a subsample of 32 individuals (6 *Pteronotus d. davyi*, 7 *P. d. incae*, and 19 *P. fulvus*). For these specimens, we collected the following external, craniodental, and mandibular measurements using digital calipers, aiming to provide information on mean and standard deviation values useful in the field and for comparisons with other bat groups:

Forearm length (FA): distance from the elbow (tip of the olecranon process) to the wrist (including the carpals). This measurement is made with the wing at least partially folded.

Occipitonasal length (OcL): greatest distance from the anteriormost projection of the nasal bones to the posteriormost portion of the occipital bone.

Condylobasal length (CBL): distance from the anteriormost projection of the premaxillae to the posteriormost projection of the exoccipital condyles.

Zygorostral length (ZygL): distance from the anteriormost projection of the premaxillae to the posteriormost projection of the postglenoid process.

Maxillary toothrow length (MXTRL): greatest crown length of the maxillary toothrow measured from the anteriormost surface of the canine to the posteriormost surface of M3.

Rostral breadth (RoB): greatest breadth across the rostrum at a right angle to the longitudinal axis of the cranium.

Interorbital breadth (InB): least width across the interorbital constriction at a right angle to the longitudinal axis of the cranium.

Anterior braincase breadth (ABB): greatest breadth across the lateral margins of the parietal at the anterior region to the suture coronalis (measured at a right angle to the longitudinal axis of the cranium).

Posterior braincase breadth (PBB): greatest breadth across the lateral margins of the parietal at the posterior region to the suture coronalis (measured at a right angle to the longitudinal axis of the cranium).

Zygomatic breadth (ZB): greatest distance across the zygomatic arches at right angle to the longitudinal axis of the cranium.

Palatal length (PL): distance from the anteriormost point of the premaxilla (excluding incisors) to the posterior margin of the horizontal process of the palatine, just in the midline of the horizontal process of the palatine.

Basioccipital breadth (BoB): least breadth across the lateral margins of the basioccipital.

M3 breadth (M3B): greatest breadth across the lateral margins of M3.

Mandibular toothrow length (MANDL): greatest distance from the anteriormost surface of i1 to the posteriormost surface of m3.

Dentary length (DENL): greatest distance from the anteriormost point of the lip of the alveolus of the lower canine to the posteriormost point of the mandibular condyle.

Mandibular depth (MAND): greatest depth of the mandibular body at the level of m2 taken at the point of greatest depth.

m2 breadth (m2B): greatest breadth across the lateral margins of m2 at a right angle to the longitudinal axis of the tooth.

m2 length (m2L): greatest length from the anteriormost point to the posteriormost point of m2.

## RESULTS

### Molecular Analyses

The cyt-*b* dataset (1140 base pairs) comprised 35 individuals and the CO1 dataset (651 bp) 50 individuals. The four specimens of *P. d. incae* had sequences for at least one of the mitochondrial markers. The molecular dataset had 147 variable positions (122 parsimony-informative sites) in the cyt-*b* dataset and 82 variable sites (67 parsimony informative) in the CO1 dataset among the three species within the subgenus *Pteronotus*. The Bayesian Inference analyses of the two separated markers recovered similar topologies showing the *P. d. incae* specimens nested within a clade comprising all individuals of *P. d. davyi* (data not shown). The concatenated dataset comprised 33 individuals, 24 of which were representatives of the subgenus *Pteronotus* and one individual of *P. d. incae*, represented by both cyt-*b* and CO1 sequences. The phylogenetic inference using the concatenated data also recovers this individual nested inside the clade of *P. davyi* (fig. 2). Table 1 shows estimates of nucleotide (Kimura-2-parameter) distances among the phylogenetic groups.

Haplotype networks inferred for both markers individually support the phylogenetic results. Three haplotype groups (clusters) are observed for each gene, corresponding to *P. fulvus*, *P. gymnonotus*, and *P. davyi*. In the cyt-*b* network (fig. 3A), 22 haplotypes were found among the 26 individuals analyzed (haplotype diversity [Hd] of 0.98): 6 haplotypes for 7 individuals of *P. gymnonotus*, 6 haplotypes for 7 individuals of *P. fulvus*, and 10 haplotypes for 12 individuals of *P. davyi*; the two individuals of *P. d. incae* sequenced for cyt-*b* share a single haplotype, which differs in one mutational step from specimens of *P. d. davyi*. The diversity for the CO1 data was slightly smaller, with 24 haplotypes observed among 38 individuals (Hd = 0.95): 6 distinct haplotypes for 11 individuals of *P. gymnonotus*, 8 haplotypes for 11 individuals of *P. fulvus*, and 10 haplotypes for 16 individuals of *P. davyi*; the three specimens of *P. d. incae* sequenced for CO1 exhibit the same haplotype, also shared with one individual of *P. d. davyi* from Saint Lucia, in the Lesser Antilles (fig. 3B).
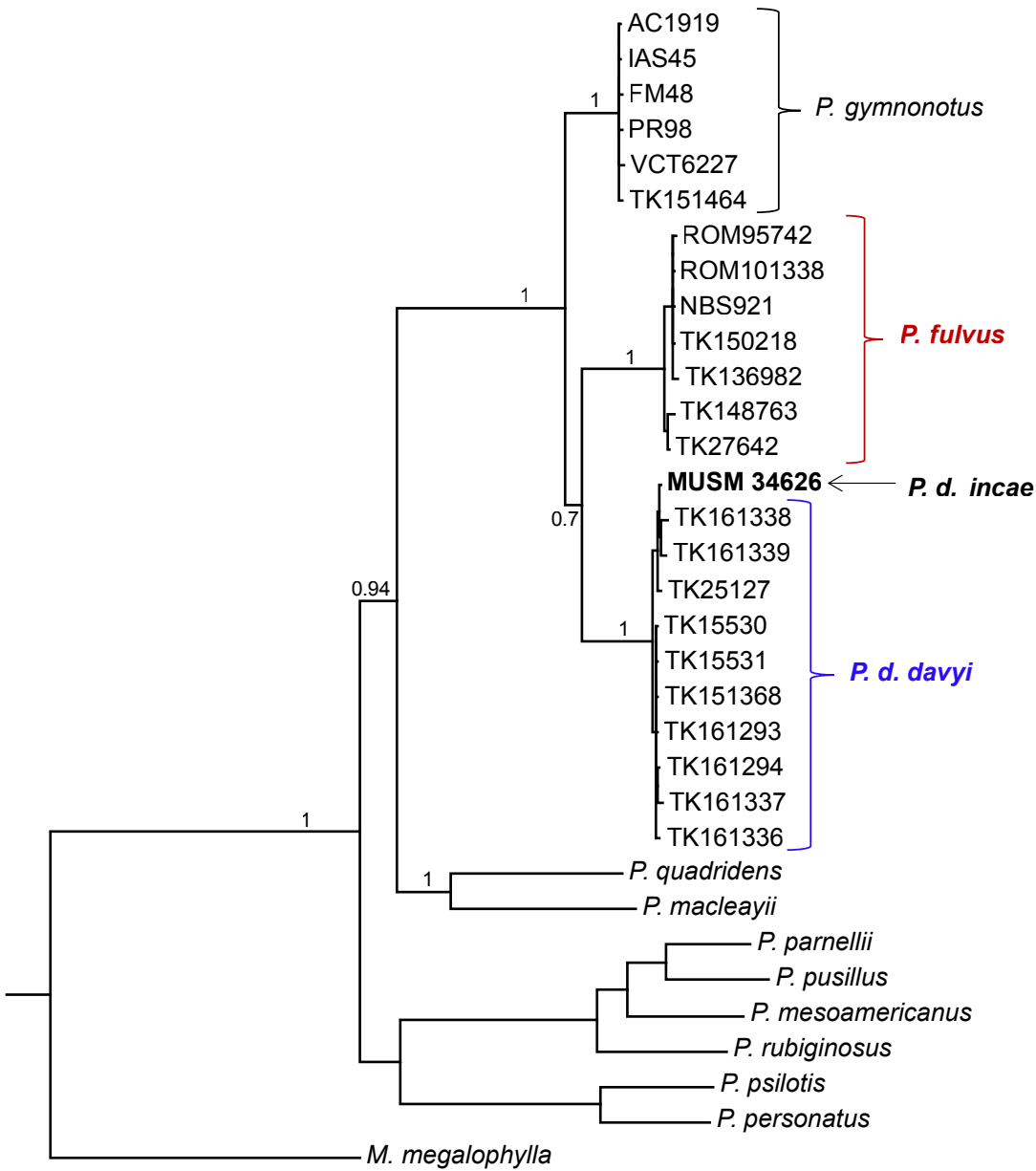
FIGURE 2. Bayesian inference phylogram using the concatenated dataset (CO1 + cyt-*b*) showing the position of the *Pteronotus d. incae* specimen (MUSM 34626) within the clade comprising all individuals of *P. d. davyi*.

TABLE 1. Nucleotide (Kimura-2-parameter) divergences of mitochondrial markers among groups defined in the subgenus *Pteronotus*. Values in black correspond to between-group distances whereas values in bold (cyt-*b*/CO1) represent within-group distances.

| | | Cyt-*b* | | | |
| --- | --- | --- | --- | --- | --- |
| | | *P. gymnonotus* | *P. fulvus* | *P. d. davyi* | *P. d. incae* |
| | *P. gymnonotus* | **0.004 / 0.002** | 0.082 | 0.071 | 0.068 |
| CO1 | *P. fulvus* | 0.060 | **0.003 / 0.005** | 0.077 | 0.076 |
| | *P. d. davyi* | 0.069 | 0.083 | **0.005 / 0.004** | 0.003 |
| | *P. d. incae* | 0.068 | 0.085 | 0.005 | **0** |

## Morphometric Analyses

Our multivariate analyses compared craniodental measurements among individuals (males and females) traditionally assigned to *P. davyi*, sensu lato. Overall, *P. fulvus* has the smallest values whereas *P. d. incae* has the largest ones; *P. d. davyi* is intermediate in size, with several variable means closer to *P. d. incae* and a few more similar to *P. fulvus*. The PCA plot (fig. 4A) highlights this pattern. The first principal component (PC1) represents a size vector and explains 60.4% of the cranial variation within the sample; the second principal component (PC2) mostly describes differences between the rostrum shape and braincase size, contributing to 8.4% of the total variation.

Multivariate analysis of variance (MANOVA) shows significant differences ($p<0.05$) in the variables between all pairwise comparisons (*P. d. davyi* × *P. d. incae*, *P. d. davyi* × *P. fulvus* and *P. d. incae* × *P. fulvus*). The MANOVA results also rejected the occurrence of significant intraspecific sexual variation within the sample (data not shown). Therefore, DFA was performed for the complete dataset, with males and females analyzed together. The DFA showed high classification rates of specimens into the defined categories (table 2): 98.4% of the specimens were correctly classified in the predicted groups; a similar value of 95.5% was observed in the jackknifed classification matrix. The DFA plot (fig. 4B) highlights the differentiation among the three categories: there is a slight overlap in the DF scores of *P. fulvus* and *P. d. davyi*, suggesting a larger similarity between them, whereas individuals of *P. d. incae* form an isolated group in the morphometric space. The first discriminant function (DF1) corresponds to 81% of the total variation and is related to size; variables with the highest loadings are associated with the expansion of the zygomatic region of the braincase.

## Morphological Analyses

Species of the subgenus *Pteronotus* share several external and craniodental characteristics: plagiopatagium attached along the median line of the body on the back, giving them the appearance of having a naked back; ears pointed, with anteromedial edge of pinnae lacking serrations; skull rostrum noticeable upturned in lateral profile; and trilobed lower incisors (Smith, 1972).

*Pteronotus gymnonotus* occurs in sympatry with some populations of *P. davyi* and *P. fulvus*. It can be easily distinguished from *P. fulvus* (FA <47 mm) by its longer forearm (FA >48 mm).
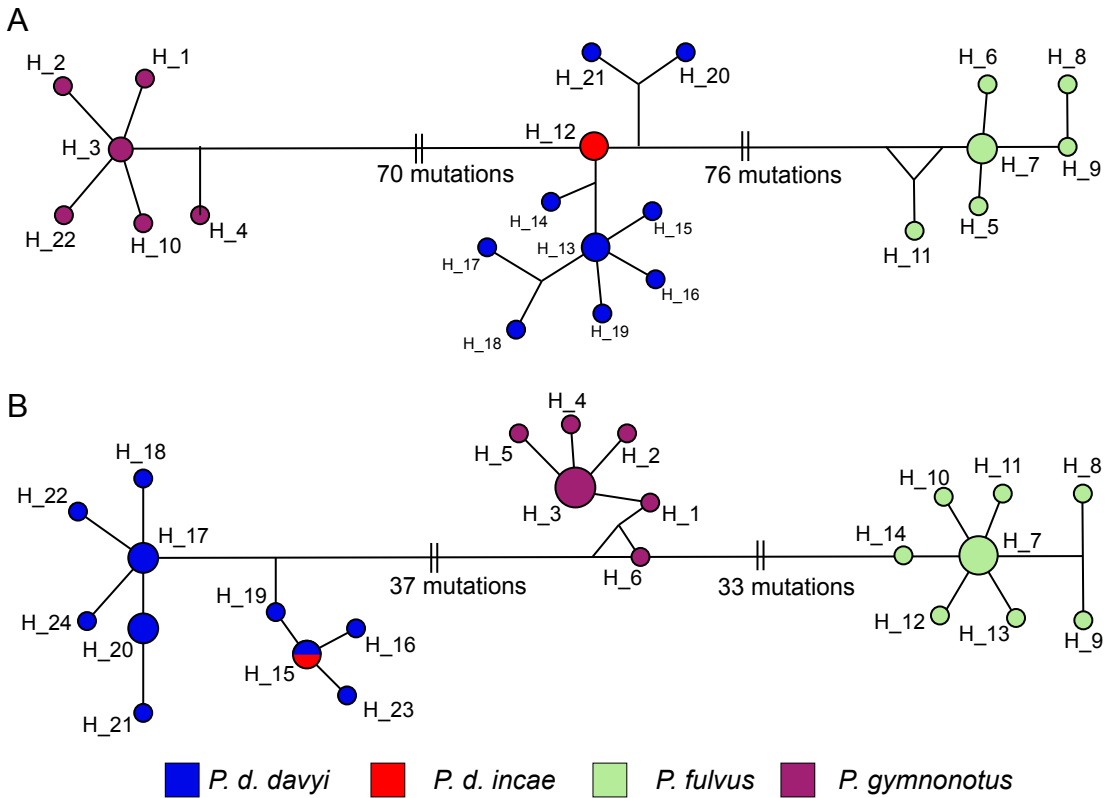
FIGURE 3. Haplotype network inferred from **A,** cyt-*b* and **B,** CO1 datasets, highlighting the clusters corresponding to *Pteronotus davyi*, *P. fulvus*, and *P. gymnonotus*. Each circle represents one distinct haplotype (H), whose size is proportional to its frequency in the sample (1 to 6 individuals).

Even though *P. gymnonotus* has substantial overlap with larger individuals of *P. davyi* (FA <51), the ventral fur on *P. gymnonotus* is unicolored, whereas it is bicolored in *P. davyi* and *P. fulvus*. The plagiopatagium covering the back of *P. gymnonotus* is covered by short and densely distributed hairs, whereas the hair in that area in *P. davyi* and *P. fulvus* is short and sparsely distributed. The rostrum in *P. gymnonotus* is conspicuously short and broad, with markedly depressed nasals, whereas the rostrum is longer with less depressed nasals in *P. davyi* and *P. fulvus*. Finally, the braincase of *P. gymnonotus* is oblong, whereas the braincase is oval in *P. davyi* and *P. fulvus* (Smith, 1972; Pavan and Tavares, 2020).

*Pteronotus davyi* and *P. fulvus*, which do not occur in sympatry, exhibit some overlap in external and craniodental measurements; with individuals of *P. davyi* tending to be larger than *P. fulvus* (table 3). *Pteronotus davyi* can be distinguished from *P. fulvus* by a grayish to reddish-brown dorsal fur (the dorsal fur ranges from dark brown to bright orange in *P. fulvus*) and bicolored ventral fur with grayish white tips (the ventral fur in *P. fulvus* is bicolored with light brown or reddish-brown tips). The rostrum is broader in *P. davyi* than in *P. fulvus*, with wider nasals and more inflated maxilla (fig. 5). The zygomatic arches are more curved in the maxillary root and the braincase is more robust in *P. davyi* as well (fig. 5). The basioccipital region

TABLE 2. Rates of correct classification of specimens in the three morphological categories (*Pteronotus ful-vus*, *P. d. davyi*, and *P. d. incae*) defined in the discriminant function analysis (DFA).

| Original classification: 98.37% | | | |
|---|---|---|---|
| | *incae* | *fulvus* | *davyi* | Total |
| *incae* | 16 | 0 | 0 | 16 |
| *fulvus* | 0 | 158 | 0 | 158 |
| *davyi* | 0 | 4 | 67 | 71 |
| Total | 16 | 162 | 67 | 245 |

| Jackknifed classification: 95.51% | | | |
|---|---|---|---|
| | *incae* | *fulvus* | *davyi* | Total |
| *incae* | 14 | 0 | 2 | 16 |
| *fulvus* | 0 | 157 | 1 | 158 |
| *davyi* | 3 | 5 | 63 | 71 |
| Total | 17 | 162 | 66 | 245 |

between the bullae is broad and almost in contact with both bullae laterally in *P. davyi*, whereas the basioccipital region between the bullae in *P. fulvus* is narrower as a result of shallow concavities on each outer edge (fig. 5). The posterior edge of the hard palate ends in an acute angle in *P. davyi*, with the lateral sides of the pterygoid bone being less divergent caudally (V-shaped), whereas it is U-shaped in *P. fulvus*. The occiput is less pronounced in *P. davyi* than in *P. fulvus*, where the occiput is more pronounced posteriorly. The two allopatric subspecies of *Pteronotus davyi* can be differentiated by the smaller size of *P. d. davyi* with respect to *P. d. incae* (table 3). Besides the differences in size, these two subspecies also show some differences in the shape of the posterior border of the hard palate, which usually is more V-shaped in *P. d. incae* (fig. 5). A summary of morphological traits distinguishing the species in the subgenus *Pteronotus* is presented in table 4.

DISCUSSION

The past five years have seen great advances in mormoopid taxonomy and systematics, but nonetheless some problems remain (Pavan and Marroig, 2016, 2017; Pavan et al., 2018). One of these problems is the taxonomic identity and phylogenetic position of *P. davyi incae* (Pavan and Marroig, 2016).

Phylogenetic analysis of mitochondrial data strongly supported the monophyly of the subgenus *Pteronotus*. However, the two molecular markers analyzed independently recover different relationships among species within the ingroup, in accordance with results previously described by Pavan and Marroig (2016). High nucleotide divergences (K2P distances between 6% and 8.5%) were observed between species, whereas low intraspecific values characterize each of the three currently recognized species of the subgenus (sensu Pavan and Marroig, 2016). The molecular data point to a high level of similarity (less than 1% divergence in the
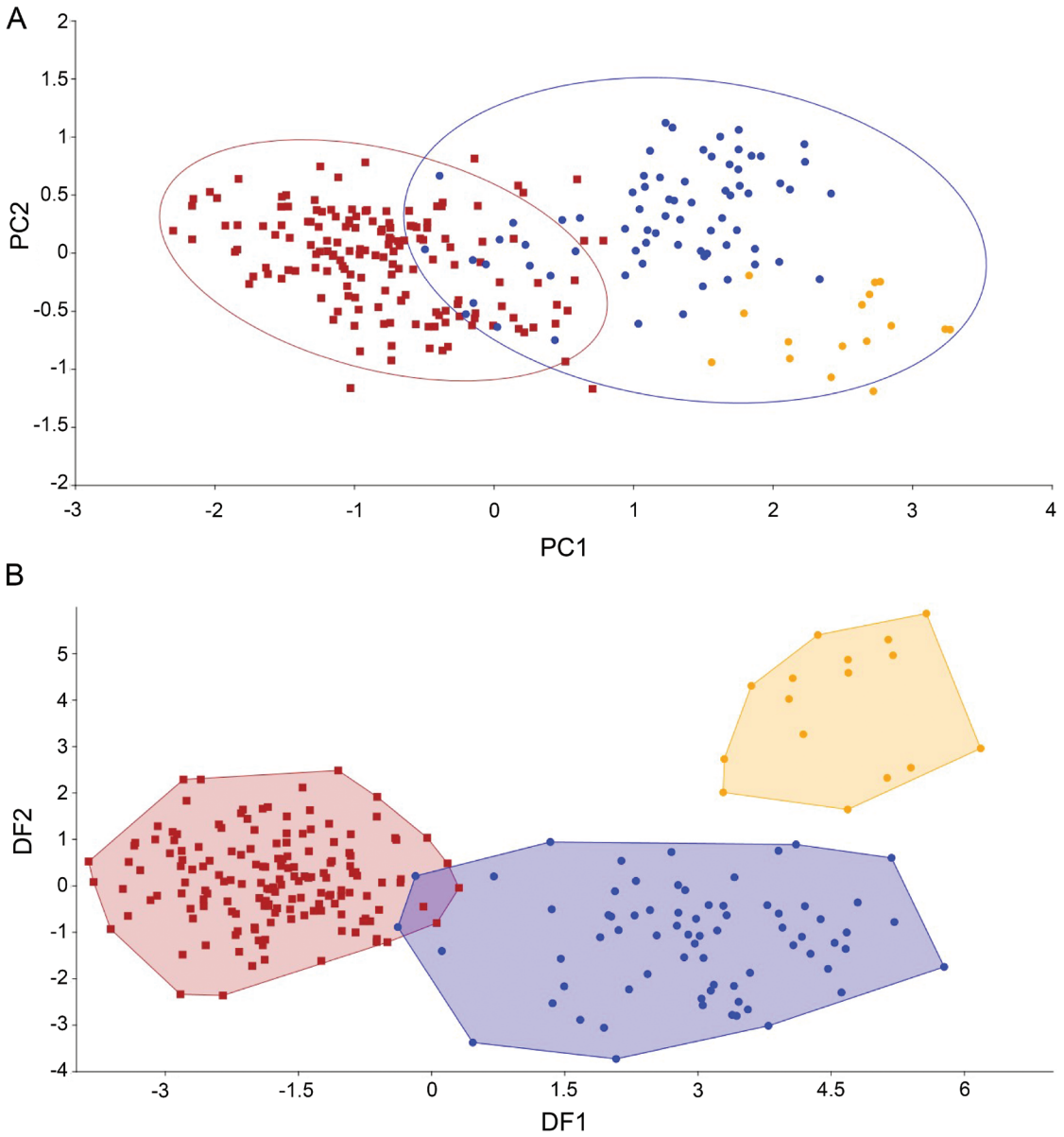
FIGURE 4. Plots of multivariate analyses showing the position of individuals of *Pteronotus fulvus* (red), *P. davyi davyi* (blue) and *P. d. incae* (orange) in the morphometric space. **A**, PCA: plot of the first and second principal components (PC1 × PC2). **B,** DFA: plot of the first and second discriminant functions (DF1 × DF2).

mitochondrial markers) between *P. davyi* samples from the Lesser Antilles islands and Peru, which represent populations of the subspecies *P. d. davyi* and *P. d. incae*, respectively. These results suggest that these two populations are not genetically distinct entities. On the other hand, our morphometric data clearly support the distinctiveness between *P. d. davyi* and *P. d. incae* in the MANOVA and no overlap in the values of several measurements (e.g., ZygL,

TABLE 3. Selected external, craniodental and mandibular measurements (mm) from 32 individuals in the *P. davyi* complex (6 *Pteronotus davyi davyi*, 7 *P. d. incae*, and 19 *P. fulvus*). Values are mean (range), number of individuals measured. See Material and Methods for abbreviations.

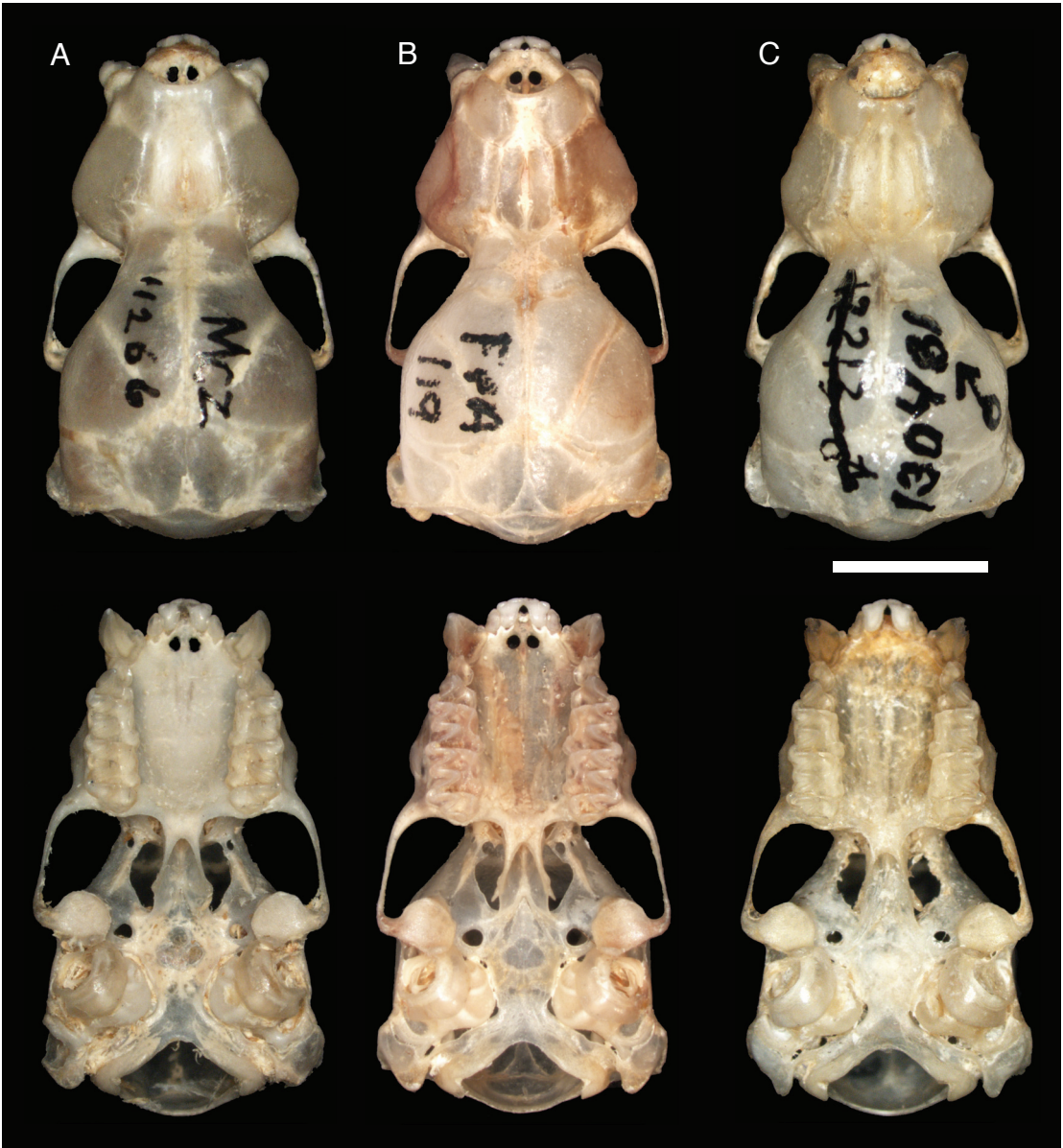| | *Pteronotus davyi davyi* | | *Pteronotus davyi incae* | | *Pteronotus fulvus* | |
|---|---|---|---|---|---|---|
| | Males | Females | Males | Females | Males | Females |
| FA | 47.5 (46.1–48.8), 3 | 46.6 (45.5–47.7), 3 | 50.2 (49.8–51.2), 5 | (49.1), 2 | 44.8 (43.4–46.7), 9 | 45.0 (44.1–45.8), 8 |
| OcL | 15.7 (15.4–16.1), 3 | 15.4 (15.3–15.5), 3 | 16.2 (15.8–16.8), 5 | (16.3), 2 | 15.1 (14.7–15.5), 10 | 15.0 (14.7–15.4), 9 |
| CBL | 15.2 (15.1–15.4), 3 | 15.0 (14.9–15.1), 3 | 15.7 (15.4–16.3), 5 | (15.8–15.9), 2 | 14.5 (14.1–14.8), 10 | 14.4 (14.1–14.6), 9 |
| ZygL | 11.0 (10.9–11.2), 3 | 11.0 (10.8–11.1), 3 | 11.5 (11.3–12.0), 5 | (11.5), 2 | 10.5 (10.2–10.9), 10 | 10.4 (10.1–10.6), 9 |
| MXTRL | (6.8), 3 | 6.7 (6.6–6.8), 3 | 7.1 (7.0–7.2), 5 | (7.0–7.1), 2 | 6.4 (6.1–6.6), 10 | 6.4 (6.2–6.6), 9 |
| RoB | 6.9 (6.9–7.1), 3 | 6.9 (6.8–7.0), 3 | 7.3 (7.1–7.6), 5 | (7.4–7.5), 2 | 6.5 (6.3–6.7), 10 | 6.6 (6.3–6.8), 8 |
| InB | 3.8 (3.7–3.9), 3 | 3.8 (3.7–3.9), 3 | 3.9 (3.7–4.0), 5 | (3.9–4.0), 2 | 3.6 (3.5–3.7), 10 | 3.6 (3.4–3.8), 9 |
| ABB | 8.1 (7.9–8.2), 3 | 8.0 (7.7–8.5), 3 | 8.2 (7.9–8.6), 5 | (8.4–8.5), 2 | 7.6 (7.3–7.9), 10 | 7.6 (7.5–7.8), 9 |
| PBB | 8.7 (8.3–9.0), 3 | (8.5–8.9), 2 | 9.4 (9.4–9.5), 3 | (9.5–9.8), 2 | 8.5 (8.3–8.8), 9 | 8.6 (8.4–8.8), 9 |
| ZB | 9.2 (9.2–9.3), 3 | 9.1 (9.0–9.3), 3 | 9.4 (9.1–9.7), 5 | (9.5–9.6), 2 | 8.6 (8.4–8.7), 9 | 8.6 (8.3–8.8), 9 |
| PL | 7.4 (7.3–7.5), 3 | 7.4 (7.3–7.5), 3 | 7.6 (7.0–8.0), 5 | (7.7–7.8), 2 | 7.1 (6.8–7.4), 10 | 7.0 (6.9–7.4), 9 |
| BoB | (1.5), 3 | 1.4 (1.4–1.5), 3 | 1.6 (1.5–1.6), 5 | (1.6), 2 | 1.3 (1.2–1.6), 10 | 1.3 (1.2–1.5), 9 |
| M3B | 1.7 (1.7–1.8), 3 | 1.8 (1.7–1.9), 3 | 1.8 (1.8–1.9), 5 | (1.8–1.9), 2 | 1.6 (1.5–1.7), 10 | 1.6 (1.5–1.7), 9 |
| MANDL | 7.8 (7.7–7.9), 3 | 7.8 (7.7–7.9), 3 | 8.2 (8.0–8.4), 5 | (8.0), 2 | 7.4 (7.3–7.6), 10 | 7.4 (6.6–7.7), 8 |
| DENL | 11.2 (11.0–11.3), 3 | 11.4 (11.3–11.6), 3 | 11.9 (11.5–12.4), 5 | (11.6–11.7), 2 | 10.9 (10.6–11.3), 10 | 10.8 (10.6–11.1), 8 |
| MAND | 1.8 (1.8–1.9), 3 | 1.7 (1.6–1.8), 3 | 1.9 (1.8–2.0), 5 | (1.9–2.0), 2 | 1.7 (1.6–1.9), 10 | 1.7 (1.6–1.8), 8 |
| m2B | (1.0), 3 | 1.0 (1.0–1.1), 3 | 1.1 (1.0–1.1), 5 | (1.0), 2 | 0.9 (0.9–1.1), 10 | 0.9 (0.9–1.0), 8 |
| m2L | (1.6), 3 | 1.6 (1.5–1.7), 3 | (1.7), 5 | (1.6–1.7), 2 | 1.5 (1.4–1.6), 10 | 1.5 (1.4–1.6), 8 |

FIGURE 5. Dorsal and ventral views of the cranium of **A,** *Pteronotus davyi davyi* (MCZ 11266, Trinidad); **B,** *P. d. incae* (MUSM 52787, Peru); and **C,** *P. fulvus* (MVZ 130481, El Salvador). Scale bar = 5 mm.

MxTRL, PBB, MANDL). The DFA result also points to consistent cranial differences between individuals currently assigned to the subspecies *davyi* and *incae*: the jackknifed classification misclassified only 3 (of 16) individuals of *P. d. incae* as belonging to *P. d. davyi*, whereas 2 (of 71) individuals of *P. d. davyi* were assigned to *P. d. incae* instead. The DFA plot shows that individuals from these two subspecies are discernible along the second discriminant function, which is mostly related to the zygomatic breadth in the skull. Our morphometric data suggest

TABLE 4. Comparison of some external and skull morphological traits among species in the subgenus *Pteronotus*.

|  | *P. fulvus* | *P. d. davyi* | *P. d. incae* | *P. gymnonotus*[1] |
|---|---|---|---|---|
| FA length | 43–47 mm | 46–49 mm | 49–51 mm | 48–55 mm[2] |
| Dorsal fur pattern | unicolored | unicolored | unicolored | mostly unicolored |
| Dorsal fur color | dark brown to bright orange | grayish to reddish-brown | grayish to reddish-brown | dark brown to bright orange |
| Ventral fur pattern | bicolored | bicolored | bicolored | unicolored |
| Ventral fur color | light brown or reddish-brown tips | grayish white tips | grayish white tips | paler than dorsal hairs |
| Hairs in the plagiopatagium | long and sparsely distributed | long and sparsely distributed | long and sparsely distributed | short and densely distributed (velvety) |
| Nasal bones | narrow and almost flattened | wide and depressed | wide and depressed | very wide and markedly depressed |
| Posterior edge of hard palate | U-shaped | V-shaped | V-shaped | V-shaped |
| Braincase shape | oval | oval | oval | oblong |
| Basioccipital region | narrower | broad | broad | remarkably broad and heart shaped |

[1] Data from Pavan and Tavares (2020).
[2] Individuals of *P. gymnonotus* with the smallest FA lengths (<50 mm) are found in the southern part of the species distribution, where *P. davyi* does not occur.

a high congruence between sets of morphological characters, which can delimit the two infraspecific categories of *P. davyi* in the discriminant space. This result is in accordance with the findings of Smith (1972), who described the subspecies *incae* based on its larger size and decidedly broader skull, particularly in the rostrum.

The contrasting results of our molecular and morphological comparisons of the populations of *P. davyi* are similar to findings in other bat taxa in which the genetic variation do not necessarily equate to patterns of morphological or geographic differentiation; as example, morphospecies once recognized in the genus *Chiroderma* and *Lasiurus* were later synonymized based on molecular evidences (Taddei and Lim, 2010; Baird et al., 2015; Garbino et al., 2020). This might reflect differing rates of morphological and molecular evolution (Wilson et al., 2013). If the Peruvian population is in fact isolated from other populations of *P. davyi*, the observed pattern of genetic homogeneity can be related to a short period of divergence from the time when gene flow between these populations was interrupted, a period insufficient for the accumulation of nucleotide differences in the mitochondrial DNA. However, the nonmonophyly in the mitochondrial genome between *P. d. davyi* and *P. d. incae* might have a specific cause: the existence of a contact zone between these populations. Current records suggest a disjunct distribution for this species in South America (Patton and Gardner, 2008; Pavan, 2019), but this might be an artifact of low population density and/or collecting effort. Records of *P. davyi* from Ecuador and southern Colombia have not been reported, and this area is key to connect populations of *P. d. davyi*, in the coastal lowlands

of Venezuela and Colombia, and *P. d. incae*, in northwestern Peru. *Pteronotus* species are generally rare in that area; in Ecuador, the only species of *Pteronotus* reported thus far is *P. rubiginosus*, which is known from only a few records from the Amazonian departments of Orellana and Sucumbios (Tirira, 2017). The reason why populations of *P. davyi* have not been reported in Ecuador or southern Colombia is not clear.

The reticulated pattern of relatedness among mitochondrial haplotypes from distinct localities of *P. davyi* also suggests that historical factors such as drift might not be the main cause of divergence in morphology, i.e., other evolutionary or ecological factors may have acted on the phenotypic variation of this species in its geographic range, as has been suggested for other taxa exhibiting such patterns (Zink, 2004). For example, Wilson et al. (2013) found strong divergence in hemoglobin amino acid substitution and body size despite considerable admixture of mtDNA and introns in populations of the Cinnamon teal (*Anas cyanoptera*) inhabiting environmental extremes. The authors suggested that neutral evolution was unlikely to generate the observed levels of divergence and concluded that selection probably had a role in the distinct populations of this species. Therefore, the geographical pattern observed in the morphology of *P. davyi* might be related to local factors acting on the individual's phenotype in different areas. We have compared some occurrence records of specimens of *P. davyi* from Peru, Venezuela, and the Lesser Antilles (the localities sampled in the morphological investigation) available on Vertnet and GBIF platforms for differences in environmental variables that could be associated with collecting localities for the two subspecies. We found that all specimens of *P. d. davyi* were captured in lowland areas (below 300 m in elevation), which would have similar temperature and humidity conditions. For *P. d. incae*, specimens have been collected at a range of different altitudes (from 200 to 2872 m), suggesting that the Peruvian population may be adapted to a wider range of climatic variables (e.g., temperature, precipitation, barometric pressure). Investigating the adaptive basis of this morphological variation and testing for correlations of morphology with environmental conditions would be necessary to fully evaluate this hypothesis.

The results of the present study show that the subspecies currently recognized within *P. davyi* do not correspond to reciprocally monophyletic groups in the mitochondrial DNA, but they do show correspondence to phenetic patterns of geographic variation. Our results suggest that gene flow has only been recently disrupted or still occurs between *P. d. davyi* and *P. d. incae*; a more detailed investigation using nuclear markers is needed for focusing on this issue. However, the view of subspecies as genealogical networks of populations, without cladistic structure, does not preclude validation of subspecies nomenclature (Patton and Conroy, 2017). The two populations of *P. davyi* have unique geographical ranges and show diagnosable phenotypic characters, two criteria that fit recognition as distinct subspecies (Braby et al., 2012). In the continuum of the speciation process (Sukumaran and Knowles, 2017), subspecies are viewed as incipient species in an allopatric scenario and might represent an adaptive response to different local environmental conditions (Braby et al., 2012). Therefore, we argue that the use of trinomials is useful in this case because they are descriptive of a geographical pattern evident in several morphological characters. Based on our findings, we there recommend continued recognition of two subspecies in *P. davyi* as currently defined (Pavan, 2019).

## SYSTEMATICS

### Family Mormoopidae Saussure, 1860

### Genus *Pteronotus* Gray, 1838

### Subgenus *Pteronotus* Gray, 1838

### *Pteronotus davyi* Gray, 1838

### Davy's Naked-backed Bat

*Pteronotus davyi* Gray, 1838: 500; type locality "Trinidad," Trinidad and Tobago.
*Chilonycteris gymnonota*: Tomes, 1863: 83; not *Chilonycteris gymnonotus* Wagner, 1843.
*Chilonycteris davyi*: Dobson, 1878: 453; name combination.
*D*[*ermonotus*]. *davyi*: Miller, 1902: 155; name combination.
*Pteronotus davyi incae* Smith, 1972: 102; type locality "4 mi W Suyo, 1000 ft, Piura," Peru.

### *Pteronotus davyi davyi* Gray, 1838

Holotype: BM 9.1.4.74 is a specimen of unknown age and sex, preserved in alcohol with the skull removed and clean. The collector and date of capture are unknown (Carter and Dolan, 1978). The type locality is the island of Trinidad, Trinidad and Tobago.

Distribution: Known from Nicaragua and Costa Rica in Central America; northern Colombia and northern Venezuela in South America; and the islands of Guadeloupe, Dominica, Martinique, Saint Lucia, Grenada, Trinidad, and Curaçao in the Lesser Antilles (fig. 1). *P. d. davyi* has also been reported based on a single individual (unvouchered to our knowledge) and acoustic data from three islands of Coiba National Park (Coiba, Jicarón, and Ranchería Islands), on the Pacific coast of Republic of Panama (Ibáñez et al., 1997; Estrada-Villegas et al., 2018), but it is absent in the continental area of Panama, which suggests a disjunct distribution for this subspecies.

Natural History: *P. d. davyi* occurs in tropical forests, woodlands, and swamps mostly at low elevations (below 400 m), showing an intimate association with dry forest and xeric shrubland habitats (Adams, 1989; Pavan, 2019). It usually forages over water and near vegetation and prefers roosting in large and warm caves, which is frequently shared with other mormoopids, phyllostomids, and natalids (Pavan, 2019). Several bat species have been reported in coexistence with populations of *P. d. davyi* along its geographic range, most notably *Pteronotus fuscus*, *P. paraguanensis*, *Mormoops megalophylla*, *Artibeus jamaicensis*, *Sturnira angeli*, *Brachyphylla cavernarum*, *Monophyllus plethodon*, *Leptonycteris curasoae*, *Glossophaga longirostris*, *Phyllostomus hastatus*, *Anoura geoffroyi*, *Carollia perspicillata*, *Noctilio leporinus*, *Molossus molossus*, *Natalus stramineus*, and *N. tumidirostris* (Goodwin and Greenhall, 1961; Genoways et al., 2001; Molinari et al., 2012; Lenoble et al., 2014), *Pteronotus d. davyi* is sensitive to ambient temperatures lower than 15° C and usually maintain a high body temperature in warm environments (Bonaccorso et al., 1992).

## *Pteronotus davyi incae* Smith, 1972

HOLOTYPE: TCWC 11638 is an adult male specimen preserved as a study skin with the skull removed and cleaned. It was collected by Dilford C. Carter (original number: 5313) on 28 July 1964 at 4 mi W of Suyo (-4.5167, -80.0667; 305 m above sea level), province of Piura, department of Piura, Peru.

DISTRIBUTION: Known only from northwestern Peru, in the departments of Cajamarca, Lambayeque, and Piura (fig. 1).

NATURAL HISTORY: *P. davyi incae* inhabits dry forest and montane forest. Lowland habitats are characterized by the presence of *Loxopterygium huasango* (Anacardiaceae); *Handroanthus chrysantha*, *Tecoma weberbaueriana* (Bignoniaceae); *Cochlospermum vitifolium* (Bixaceae); *Ceiba trichistandra*, *Eriotheca ruizii* (Malvaceae); *Cordia lutea*, *Cordia peruviana* (Boraginaceae); *Bursera graveolens* (Burseraceae); *Colicodendron scabridum* (Capparaceae); *Ipomoea carnea*, *Ipomoea philomega* (Convolvulaceae); *Muntingia calabura* (Muntingiaceae); *Acacia macracantha*, *Pithecellobium multiflorum*, *Prosopis pallida* (Fabacea); *Psittacanthus tumbecensis* (Loranthaceae); and *Ficus jacobii* (Moraceae) (Leal-Pinedo and Linares Palomino, 2005; Linares-Palomino and Ponce-Alvarez, 2005; Linares-Palomino and Pennington, 2007; Odar 2010). Lowland populations of *P. d. incae* occur in sympatry with *Artibeus fraterculus*, *Desmodus rotundus*, *Glossophaga soricina*, *Lonchophylla hesperia*, *Lophostoma occidentalis*, *Phylloderma stenops*, *Phyllostomus discolor*, *Sturnira bakeri*, *Eptesicus innoxius*, and *Molossus molossus* (Pacheco et al., 2009; Velazco and Cadenillas, 2011). Individuals from San Ignacio and Yaquil (MUMS 52786, 52787) were captured in a double-high mist-nest system, both at 4.5 meters above ground, and individuals from Salitral-Huarmanca (MUSM 34625, 34626) were collected at 4 meters, one with a high mist net system and the other with a shotgun.

## ACKNOWLEDGMENTS

## REFERENCES

Adams, J.K. 1989. *Pteronotus davyi*. Mammalian Species 346: 1–5.

Baird, A.B., et al. 2015. Molecular systematic revision of tree bats (Lasiurini): doubling the native mammals of the Hawaiian Islands. Journal of Mammalogy 96: 1255–1274.

Bandelt, H.J., P. Forster, and A. Röhl. 1999. Median-joining networks for inferring intraspecific phylogenies. Molecular Biology and Evolution 16: 37–48.

Bonaccorso, F.J., et al. 1992. Thermal ecology of moustached and ghost-faced bats (Mormoopidae) in Venezuela. Journal of Mammalogy 73: 365–378.

Braby, M. F., Eastwood, R., and N. Murray. 2012. The subspecies concept in butterflies: has its application in taxonomy and conservation biology outlived its usefulness? Biological Journal of the Linnean Society 106: 699–716.

Carter, D.C., and P.G. Dolan. 1978. Catalog of type specimens of Neotropical bats in selected European museums. Special Publications, Museum Texas Tech University 15: 1–136.

Dávalos, L.M., 2006. The geography of diversification in the mormoopids (Chiroptera: Mormoopidae). Biological Journal of the Linnean Society 88: 101–118.

Estrada-Villegas, S., et al. 2018. Bats and their bat flies: community composition and host specificity on a Pacific island archipelago. Acta Chiropterologica 20: 161–176.

Garbino, G.S.T., B.K. Lim, and V.d.C. Tavares. 2020. Systematics of big-eyed bats, genus *Chiroderma* Peters, 1860 (Chiroptera: Phyllostomidae). Zootaxa 4846: 1–93.

Genoways, H.H., et al. 2001. Bats of the West Indian island of Dominica: natural history, areography, and trophic structure. Special Publications, Museum of Texas Tech University 43: 1–43.

Goodwin, G.G., and A.M. Greenhall. 1961. A review of the bats of Trinidad and Tobago: descriptions, rabies infection, and ecology. Bulletin of the American Museum of Natural History 122: 187–302.

Hammer, Ø., D.A.T. Harper, and P.D. Ryan. 2001. PAST: Paleontological statistics software package for education and data analysis. Palaeontologia Electronica 4: 1–9.

Herd, R.M. 1983. *Pteronotus parnellii*. Mammalian Species 209: 1–5.

Ibáñez, C., J.L. Pérez-Jordá, J. Juste B., and A. Guillén. 1997. Los mamíferos terrestres del Parque Nacional de Coiba (Panamá). *In* S. Castroviejo and M. Velayos (editors), Flora y Fauna del Parque Nacional de Coiba (Panamá): inventario preliminar: 471–484. Madrid: Agencia Española de Cooperación Internacional.

Leal-Pinedo, J.M., and R. Linares-Palomino. 2005. Los bosques secos de la Reserva de Biosfera del Noroeste (Diversidad arbórea y estado de conservación). Caldasia 27: 195–211.

Lenoble A., et al. 2014. Predation of lesser naked-backed bats (*Pteronotus davyi*) by a pair of American kestrels (*Falco sparverius*) on the island of Marie-Galante, French West Indies. Journal of Raptor Research 48: 78–81.

Librado, P., and J.Rozas. 2009. DNAsp v.5: a software for comprehensive analysis of DNA polimorphism data. Bioinformatics 25: 1451–1452.

Linares-Palomino, R., and R.T. Pennington. 2007. Lista anotada de plantas leñosas en bosques estacionalmente secos del Perú: una nueva herramienta en Internet para estudios taxonómicos, ecológicos y de biodiversidad. Arnaldoa 14: 149–152.

Linares-Palomino, R., and S.I. Ponce-Alvarez. 2005. Tree community patterns in seasonally dry tropical forests in the Cerros de Amotape Cordillera, Tumbes, Peru. Forest Ecology and Management 209: 261–272.

Molinari, J., et al. 2012. Singularidad biológica e importancia socioeconómica de los murciélagos cavernícolas de la península de Paraguaná, Venezuela, con propuestas para su conservación. Revista de Ecología Latinoamericana 17: 1–40.

Odar, J. 2010. Especies forestales del Coto de Caza el Angolo Sullana-Piura. Bachelor's thesis, Universidad Nacional de Piura, Peru.

Pacheco, V., Cadenillas, R., Salas, E., Tello, C., and H. Zeballos. 2009. Diversidad y endemismo de los mamíferos del Perú. Revista Peruana de Biología 16: 5–32.

Patton, J.L., and C.J. Conroy. 2017. The conundrum of subspecies: morphological diversity among desert populations of the California vole (*Microtus californicus*, Cricetidae). Journal of Mammalogy 98: 1010–1026.

Patton, J.L., and A.L. Gardner. 2008. Family Mormoopidae. *In* A.L. Gardner (editor), Mammals of South America, vol. 1. Marsupials, xenarthrans, shrews, and bats: 376–384. Chicago: University of Chicago Press.

Pavan, A.C. 2019. Family Mormoopidae (ghost-faced bats, naked-backed bats and mustached bats). *In* D.E. Wilson and R.A. Mittermeier (editors.), Handbook of the mammals of the world. Barcelona: Lynx Edicions.

Pavan, A.C., and G. Marroig. 2016. Integrating multiple evidences in taxonomy: species diversity and phylogeny of mustached bats (Mormoopidae: *Pteronotus*). Molecular Phylogenetics and Evolution 103: 184–198.

Pavan, A.C., and G. Marroig. 2017. Timing and patterns of diversification in the Neotropical bat genus *Pteronotus* (Mormoopidae). Molecular Phylogenetics and Evolution 108: 61–69.

Pavan, A.C., and V.d.C. Tavares. 2020. *Pteronotus gymnonotus* (Chiroptera: Mormoopidae). Mammalian Species 52 (990): 40–48.

Pavan, A.C., P.E.D. Bobrowiec, and A.R. Percequillo. 2018. Geographic variation in a South American clade of mormoopid bats, *Pteronotus* (*Phyllodia*), with description of a new species. Journal of Mammalogy 99: 624–645.

Rambaut, A., M.A. Suchard, D. Xie, and A.J. Drummond. 2014. Tracer v1.6, online resource (http://beast.bio.ed.ac.uk/Tracer).

Ronquist, F., and J.P. Huelsenbeck. 2003. MrBayes 3: Bayesian phylogenetic inference under mixed models. Bioinformatics 19: 1572–1574.

Ronquist, F., J.P. Huelsenbeck, and M. Teslenko. 2011. MrBayes version 3.2 manual: tutorials and model summaries.

Smith, J.D. 1972. Systematics of the chiropteran family Mormoopidae. Miscellaneous Publications, Museum of Natural History, University of Kansas 56: 1–132.

Sukumaran, J., and L.L. Knowles. 2017. Multispecies coalescent delimits structure, not species. Proceedings of the National Academy of Sciences of the United States of America 114: 1607–1612.

Taddei, V.A., and B.K. Lim. 2010. A new species of *Chiroderma* (Chiroptera, Phyllostomidae) from northeastern Brazil. Brazilian Journal of Biology 70: 381–386.

Tamura, K., G. Stecher. D. Peterson, A. Filipski, and S. Kumar. 2013. MEGA6: molecular evolutionary genetics analysis, version 6.0. Molecular Biology and Evolution 30: 2725–2729.

Tirira, D.G. 2017. Guía de campo de los mamíferos del Ecuador, segunda edición. Publicación especial sobre los mamíferos del Ecuador 11. Quito: Ediciones Murciélago Blanco.

Velazco, P.M., and R. Cadenillas. 2011. On the identity of *Lophostoma silvicolum occidentalis* (Davis & Carter, 1978) (Chiroptera: Phyllostomidae). Zootaxa 2962: 1–20.

Wilson, R.E., J.L. Peters, and K.G. McCracken. 2013. Genetic and phenotypic divergence between low- and high-altitude populations of two recently diverged cinnamon teal subspecies. Evolution 67: 170–184.

Zink, R.M., 2004. The role of subspecies in obscuring avian biological diversity and misleading conservation policy. Proceedings of the Royal Society of London B, Biological Sciences 271: 561–564.

## APPENDIX 1

### Specimens Used in Molecular Analyses

Specimens included in the molecular dataset, showing the availability of sequence data for cytochrome *b* (cyt-*b*) and cytochrome oxidase I (CO1), with data on their localities and GenBank Accession numbers. See Material and Methods for abbreviations.

| Museum | ID | Species | Locality | Country | cyt-*b* | CO1 | GenBank accession number(s) |
|---|---|---|---|---|---|---|---|
| MUSM | 34625 | *P. d. incae* | Piura | Peru | | X | MW526427 |
| MUSM | 34626 | *P. d. incae* | Piura | Peru | X | X | MW526430, MW526428 |
| MUSM | 52786 | *P. d. incae* | Cajamarca | Peru | | X | MW526429 |
| MUSM | 52787 | *P. d. incae* | Cajamarca | Peru | X | | MW526431 |
| TTU | TK25127 | *P. d. davyi* | Nariva | Trinidad | X | X | AF338671, KX590177 |
| TTU | TK15530 | *P. d. davyi* | St. John | Dominica | X | X | KX589876, KX590175 |
| TTU | TK15531 | *P. d. davyi* | St. Paul | Dominica | X | X | KX589877, KX590176 |
| TTU | TK151288 | *P. d. davyi* | Castries | Saint Lucia | | X | KX590182 |
| TTU | TK151368 | *P. d. davyi* | Castries | Saint Lucia | X | X | KX589881, KX590183 |
| TTU | TK151370 | *P. d. davyi* | Castries | Saint Lucia | | X | KX590185 |
| TTU | TK161179 | *P. d. davyi* | Praslin | Saint Lucia | | X | KX590186 |
| TTU | TK161214 | *P. d. davyi* | Micoud | Saint Lucia | | X | KX590187 |
| TTU | TK161215 | *P. d. davyi* | Micoud | Saint Lucia | | X | KX590188 |
| TTU | TK161247 | *P. d. davyi* | Soufriere | Saint Lucia | | X | KX590189 |
| TTU | TK161293 | *P. d. davyi* | Micoud | Saint Lucia | X | X | KX589885, KX590190 |
| TTU | TK161294 | *P. d. davyi* | Micoud | Saint Lucia | X | X | KX589886, KX590191 |
| TTU | TK161336 | *P. d. davyi* | Castries | Saint Lucia | X | X | KX589887, KX590192 |
| TTU | TK161337 | *P. d. davyi* | Castries | Saint Lucia | X | X | KX589888, KX590193 |
| TTU | TK161338 | *P. d. davyi* | Castries | Saint Lucia | X | X | KX589889, KX590194 |
| TTU | TK161339 | *P. d. davyi* | Castries | Saint Lucia | X | X | KX589890, KX590195 |
| ROM | 95742 | *P. fulvus* | Campeche | Mexico | X | X | KX589859, JF447313 |
| TTU | TK148763 | *P. fulvus* | Jalisco | Mexico | X | X | KX589879, KX590180 |
| TTU | TK150218 | *P. fulvus* | Chiapas | Mexico | X | X | KX589880, KX590181 |
| TTU | TK27642 | *P. fulvus* | Jalisco | Mexico | X | X | AF338672, KX590178 |
| ROM | 99291 | *P. fulvus* | El Peten | Guatemala | | X | JF446816 |
| ROM | 98424 | *P. fulvus* | Alta Verapaz | Guatemala | | X | JF446821 |
| ROM | 101338 | *P. fulvus* | Ahuachapan | El Salvador | X | X | KX589864, JF446542 |
| ROM | 101305 | *P. fulvus* | Ahuachapan | El Salvador | | X | JF446541 |
| AMNH | NBS921 | *P. fulvus* | Orange Walk District | Belize | X | X | KX589762, KX590084 |
| AMNH | NBS922 | *P. fulvus* | Orange Walk District | Belize | | X | KX590085 |

APPENDIX 1 *continued*

| Museum | ID | Species | Locality | Country | cyt-*b* | CO1 | GenBank accession number(s) |
|--------|-----|---------|----------|---------|---------|-----|------------------------------|
| TTU | TK136982 | *P. fulvus* | Colon | Honduras | X | X | KX589878, KX590179 |
| UFPB | AF487 | *P. gymnonotus* | Aiuaba, Ceará | Brazil | | X | KX590285 |
| MZUSP | FM48 | *P. gymnonotus* | Jangada, Mato Grosso | Brazil | X | X | KX589842, KX590156 |
| UFPB | PR98 | *P. gymnonotus* | Itabaiana, Sergipe | Brazil | X | X | KX589983, KX590304 |
| UFRJ | IAS23 | *P. gymnonotus* | Chapada Diamantina, Bahia | Brazil | | X | KX590309 |
| UFRJ | IAS45 | *P. gymnonotus* | Chapada Diamantina, Bahia | Brazil | X | X | KX589988, KX590310 |
| MZUSP | AC1919 | *P. gymnonotus* | FLONA Tapirapé-Aquiri, Pará | Brazil | X | X | KX589826, KX590140 |
| UFMG | VCT6227 | *P. gymnonotus* | FLONA Carajás, Pará | Brazil | X | X | KX590035, KX590354 |
| UFMG | VCT6399 | *P. gymnonotus* | FLONA Carajás, Pará | Brazil | | X | KX590368 |
| UFMG | VCT6407 | *P. gymnonotus* | FLONA Carajás, Pará | Brazil | | X | KX590370 |
| UFMG | VCT6409 | *P. gymnonotus* | FLONA Carajás, Pará | Brazil | | X | KX590372 |
| TTU | TK151464 | *P. gymnonotus* | Brokopondo | Suriname | X | X | KX589892, KX590198 |
| TTU | TK22845 | *P. gymnonotus* | Huanuco | Peru | X | | AF338674 |
| TTU | TK27697 | *P. quadridens* | St. Ann Parish | Jamaica | X | X | KX589951, KX590268 |
| AMNH | LDM132 | *P. macleayii* | St. Catherine Parish | Jamaica | X | X | AY604461, KX590079 |
| TTU | TK27683 | *P. parnellii* | St. Ann Parish | Jamaica | X | X | KX589906, KX590212 |
| AMNH | AT58 | *P. pusillus* | Maria Trinidad Sanchez | Dominican Republic | X | X | KX589749, KX590057 |
| IEPA | 554 | *P. rubiginosus* | P.N.Tumucumaque, Amapá | Brazil | X | X | KF636804, KF636800 |
| TTU | TK14516 | *P. mesoamericanus* | San Luis Potosi | Mexico | X | X | KX589896, KX590203 |
| MZUSP | AC1515 | *P. personatus* | FLONA Tapirapé-Aquiri, Pará | Brazil | X | X | KX589818, KX590133 |
| TTU | TK12043 | *P. psilotis* | Oaxaca | Mexico | X | X | AF338680, KX590265 |
| TTU | TK27640 | *M. megalophylla* | Jalisco | Mexico | X | X | AF330808, JF446806 |

APPENDIX 2

Specimens used in the morphometric investigation with data on their respective localities and coordinates. See Material and Methods for abbreviations.

*Pteronotus davyi davyi.* **COSTA RICA (4)**––*Alajuela*: 8.4 mi W Atenas (LACM 25640, 25641): 9.98 -84.45. *Guanacaste*: Playas del Coco (LACM 23732): 10.55 -85.71; Liberia, 5 mi N (LACM 26531): 10.71 -85.43. **DOMINICA (11)**–– (FMNH 44260): 15.5 -61.33; Roseau (NMNH 113190): 15.3 -61.4; Belvedeer Estate (NMNH 113573, 113592): 15.28 -61.25; Grand Bay (NMNH 361894, 391218): 15.23 -61.32; South Chiltern (NMNH 361895, 362096): 15.25 -61.37. *St. Joseph*: 1 mi above mouth Layou River (TTU 31327): 15.41 -61.43. *St. Paul*: Antrim Valley (TTU 31305, 31328): 15.35 -61.38. **NICARAGUA (18)**––*Matagalpa*: 3 mi E San Ramon (KU 70333, 70334, 70337, 70415, 70416, 70418, 70419, 70421, 70423, 70425, 70427, 70428, 70431, 70433, 70434, 70435, 70436, 70442): 12.92 -85.79. **TRINIDAD AND TOBAGO (4)**–– *Caroni*: (NMNH 399559): 10.6 -61.38. *Mayaro*: Guayaguayare (TTU 5227): 10.13 -61.03. *St. George*: Cuara Valley (TTU 5497):10.7 -61.35; Blanchisseuse (TTU 9775): 10.78 -61.3. **VENEZUELA (34)**––*Aragua*: 3 km S Ocumare de La Costa (NMNH 517293, 517294): 10.4 -67.77; El Limon, 4 km NW Maracay (NMNH 517295, 517296): 10.28 -67.6. *Falcon*: 7 km W Pueblo Nuevo, Peninsula de Paraguaná (NMNH 444125, 444126, 444128, 444130, 444131, 444143, 444144, 444145, 444154): 11.93 -69.98. *Lara*: 10 km N El Tocuyo (Casserio Boro) (NMNH 444164): 9.88 -69.78. *Vargas*: Hda. Carapiche, near El Limon, 48 Km W Caracas (NMNH 385285): 10.48 -67.32. *Yaracuy*: 8 km N 18 km W San Felipe (NMNH 418749): 10.43 -68.91; Minas de Aroa (NMNH 418761, 418762, 418764, 418769–418778, 418781–418784, 418786): 10.43 -68.9.

*Pteronotus davyi incae.* **PERU (16)**––*Cajamarca*: Jaen (AMNH 69233): -5.7 -78.78; San Ignacio (MUSM 52786): -5.17 -78.95; Chota, Conchan, Yaquil (MUSM 52787): -6.46 -78.69. *Piura*: 4 mi W Suyo, 1000 ft (TCWC 11639, 11640): -4.51 -80.06; Hacienda Bigote (FMNH 81034, 81035, 81037–81042): -5.32 -79.8; Huancabamba (AMNH 64082): -5.23 -79.46; ACR Bosques Secos de Salitral-Huarmaca (MUSM 34625, 34626): -5.46 -79.79.

*Pteronotus fulvus.* **BELIZE (10)**––*Cayo*: Ontario Village (FMNH 108738): 17.22 -88.88; Central Farm, along Garbutts Creek (FMNH 58139): 17.19 -89. *Orange Walk*: Tower Hill, Belize Sugar Industries Compound (FMNH 108740): 18.03 -88.55; Tower Hill, Belize Sugar Industries Swim Pool (FMNH 58140, 58141): 18.03 -88.55. *Stann Creek*: Cockscomb basin wildlife sanctuary, 80 m (NMNH 583006): 16.77 -88.53. *Toledo*: Agriculture Station, Punta Gorda Road (FMNH 108735): 16.13 -88.83; San Antonio (FMNH 108736): 16.24 -89.02; Agriculture Station (FMNH 108737): 16.13 -88.83; Punta Gorda, San Antonio road, 1/4 mi W Agri Sta (FMNH 108741): 16.13 -88.84. **GUATEMALA (18)**––*Alta Verapaz*: Lanquin cave, 1022 ft (FMNH 64466; KU 64793–64796, 64669, 64756–64766): 15.57 -89.98. *Chiquimula*: Jocotan, near Chiquimula, 1350 ft (KU 84091): 14.82 -89.38. **HONDURAS (12)**––*Santa Barbara*: 2 km S San Nicholas, 660 m (TCWC 18665–18676): 14.91 -88.32. **MEXICO (118)**––*Campeche*: 5 km S Champotón, 10 m (KU 91498, 91499): 19.28 -90.73; 12 km W Escarcega (KU 91500, 91501, 93236, 93237): 18.61 -90.86; 105 km E Escarcega (KU 93241): 18.58 -89.74. *Chiapas*: 13 mi SW Las Cruces (KU 68632, 68633, 68635, 68636, 68638, 70332): 16.19 -93.97. *Colima*: 7 mi W, 0.5 mi S Santiago (KU 36433, 36435, 36437–36439, 36441, 36442, 36460, 36462, 36463): 19.12 -104.46; Playa de Oro, 8 km W, 2 km S Santiago (KU 87303, 87304): 19.1 -104.44. *Guerrero*: 2 mi NW Acapulco, 50 ft (KU 38205, 38206, 38208–38210,

38212–38215): 16.88 -99.94; 10 mi E, 2 mi S Teloloapan (KU 66318, 66319, 66322): 18.34 -99.71. *Jalisco*: 5 mi S El Grullo, 3100 ft (KU 103382): 19.73 -104.23; 15 km W Ameca, 4200 ft (KU 92709): 20.55 -104.2; Chamela (TTU 45007): 19.53 -105.07. *Michoacan*: 7 mi S Tumbiscatio, 2700 ft (KU 39497): 18.42 -102.39. *Nayarit*: 2 mi S Compostella, 2900 ft (KU 39496): 21.2 -104.91. *Oaxaca*: Santo Domingo Tehuantepec (AMNH 165952): 16.33 -95.23. *San Luis Potosi*: El Salto falls (AMNH177590, 177592, 177593, 177597, 177599–177610, 177611, 178078): 22.58 -99.38. *Sinaloa*: 1 mi S, 6 mi E El Carrizo (KU 105426, 105427): 26.25 -108.94; 1 mi E Santa Lucia, 5650 ft (KU 67319): 23.44 -105.83; 1 mi E Sinaloa, 180 ft (KU 89999): 25.84 -108.19; Panuco, 2050 ft (KU 95712, 95714–95720): 23.42 -105.91; 3 mi SE Plomosas, 4000 ft (KU 96959): 23.03 -105.47; 17 mi NE Elota, 200 ft (TCWC 7510): 24.09 -106.6. *Sonora*: Carbo, 14.9 mi SE; Cueva del Tigre (LACM 12401, 12403, 12404, 12406, 12407): 29.47 -110.92; 13 mi S Carbo, 1200 ft (TCWC 7511, 7514, 7516, 7517): 29.5 -110.96. *Tamaulipas*: Rancho Santa Rosa, 25 km N, 13 km W Cd Victoria, 260 m (KU 57528–57531, 57534): 23.96 -99.31; Rancho Pano Ayuctle 6 mi N Gomez Farias, 300 m (KU 60248): 23.11 -99.16. *Veracruz*: 3 km E San Andres Tuxtla, 1000 ft (KU 23577–23579, 23581–23586, 23633, 23634; TCWC 9055–9063, 9071–9073): 18.46 -95.19. *Yucatan*: 3 km S, 1 km W Calcehtoc, Cueva de Oxkintoc (TTU 18413, 18414): 20.54 -89.92; Cueva de Hoctum, 1 km S Hoctun (TTU 25884, 25885): 20.86 -89.2; 6 km S, 5 km W Kinchil (TTU 25886): 20.86 -90.